Application note | 002821

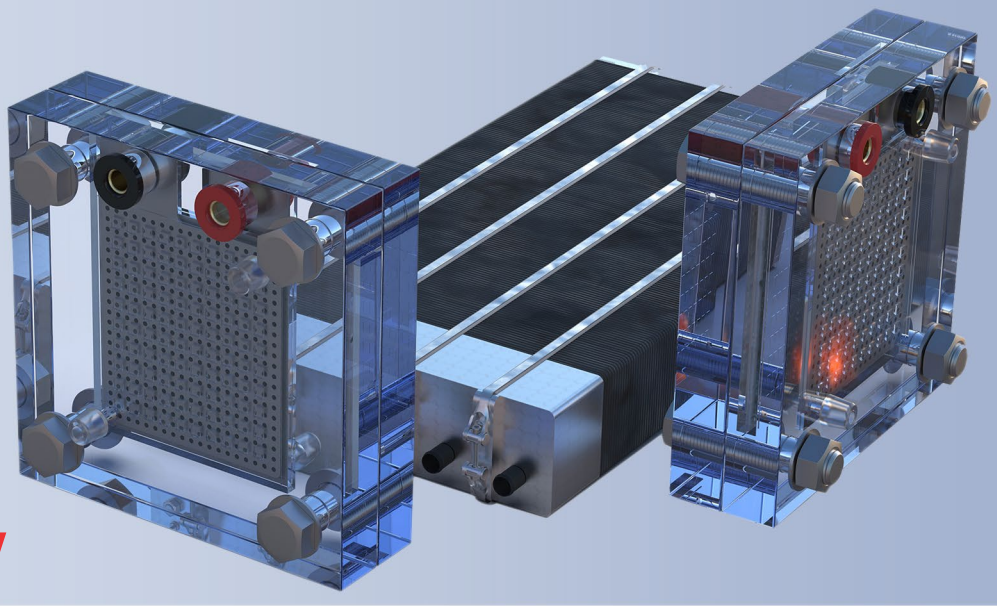

Industrial

Analysis of process water from hydrogen fuel cells using triple quadrupole inductively coupled plasma mass spectrometry (ICP-MS)

Authors

Tomoko Vincent, Bhagyesh Surekar, and Daniel Kutscher

Thermo Fisher Scientific, Bremen, Germany

Keywords

Fluorine, fuel cell, high resolution, ICP-MS, KED, PEM, process water, triple quadrupole, TQ-O_2 mode

Goal

To demonstrate the analysis of process water from hydrogen fuel cells for inorganic trace contaminants with high sensitivity and accuracy using triple quadrupole ICP-MS

Introduction

The reduction of CO_2 emissions is a major task for societies globally as the rise of CO_2 in the atmosphere plays an enormous role in global warming. The automotive industry mainly focuses on the transition from petrol-fueled to electric vehicles (EVs) to reduce emissions; however, the generation of energy and energy-intensive industrial processes are also important sources of emissions. Here, other ways of reducing CO_2 emissions might be feasible, and in the center of current debate stands the use of (ideally green) hydrogen and its combustion in hydrogen fuel cells. Hydrogen fuel cells are one of the key technological developments as there is no emission other than water. In addition, hydrogen can be created using renewable energies and can be transported with low effort due to its low density of only 70.85 $g \cdot L^{-1}$ when liquified.

A typical hydrogen fuel cell consists of two electrodes (anode and cathode) and a polymeric electrolyte membrane (PEM) as shown in Figure 1. Typically, the electrode is made from fluorinated polymers to allow for chemical and mechanical stability and coated with a catalyst. Platinum is the catalyst material offering the highest efficiency; however, it is expensive. To reduce the production cost, improving the platinum coating technology and monitoring potential degradation by means of metal release into the water produced in the process are important. Due to the use of material blends, different trace metals as well as other non-metal contaminants must be monitored.

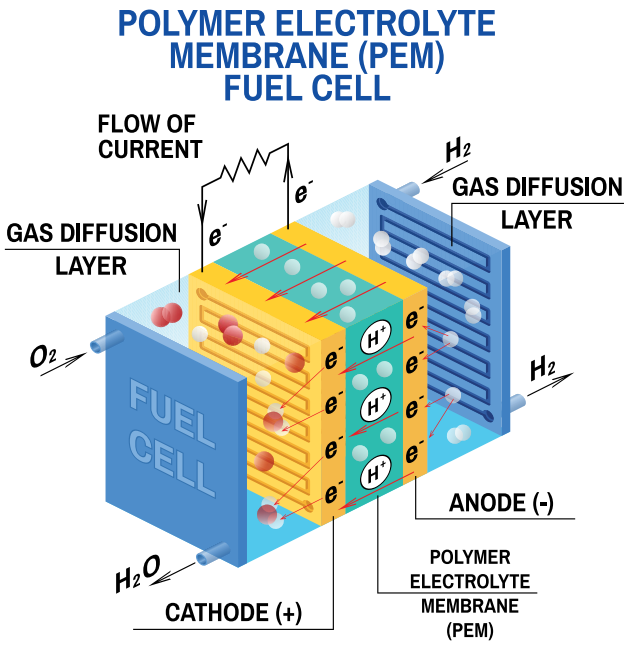

Figure 1. Hydrogen fuel cell diagram

In general, inductively coupled plasma mass spectrometry (ICP-MS) is the preferred analytical technique for the analysis of metals and related contaminants down to sub ng·L^{-1} levels. However, non-metals such as phosphorous or sulfur are challenging to analyze using ICP-MS due to a combination of their usually elevated ionization potentials and significant spectral interferences. Current hydrogen fuel cell technology uses mineral acids, like sulfuric acid, as electrolytes with a platinum catalyst on the electrodes (PAFC). Thus, it is important to monitor the concentrations of these elements at low concentrations. Oxygen- and nitrogen-based polyatomic interferences are usually of greatest concern for these analytes, but other polyatomic interference, like $^{31}P^{1}H^{+}$, may lead to false positive results and must be removed.

Another challenge is the analysis of fluorine, which is also a key analyte for monitoring degradation of the PEM. Fluorine has the third highest first ionization potential of any element in the periodic table (behind neon and helium). In addition, its only naturally occurring isotope, ^{19}F, falls into a severely interfered mass range, mainly due to the interferences generated by naturally abundant ions such as H_3O^+ and peak tailing of H_2O^+. To overcome these challenges, fluorine can be measured indirectly after mixing the sample with a solution containing barium. This results in the formation of $^{138}Ba.^{19}F^+$ in the plasma, allowing the fluorine concentration to be measured interference free via *m/z* 157. Because of the required setup, the analysis of fluorine has to be conducted in a separate measurement and cannot be combined with the analysis of the other contaminants.

In this study, a Thermo Scientific™ iCAP™ TQe ICP-MS was used for the analysis. Use of triple quadrupole technology offered superior interference removal and facilitated the analysis of important contaminants, including fluorine, at ultra-trace levels in the water produced by hydrogen fuel cells.

Experimental

Experimental optimization of the instrument parameters

An iCAP TQe ICP-MS, operated together with a Thermo Scientific™ iSC-65 Autosampler, was used for all analyses. The sample introduction system components used in these experiments are summarized in Table 1. In addition to O_2 in triple quadrupole mode for highly interfered analytes such as sulfur, phosphorous, arsenic, and selenium, the instrument was also operated in single quadrupole mode using helium and kinetic energy discrimination (KED) for interference-free analysis of other measured analytes over the full mass range. Table 1 summarizes the instrument configuration and analytical parameters. The selection of the most appropriate isotopes per analyte, as well as the optimum analysis conditions (i.e., KED mode versus reactive gas, on mass mode versus mass shift reaction mode) was automatically accomplished using the Reaction Finder Method Development Assistant available in the Thermo Scientific™ Qtegra™ Intelligent Scientific Data Solution™ (ISDS) Software. Measurement modes were optimized using the provided autotune procedures.

The iSC-65 Autosampler allowed for the use of Step Ahead feature to shorten the overall measurement time per sample and increase the productive time of the instrument.

Table 1. Instrument configuration and operating parameters

Instrument parameter	Value (general analysis)		Value (fluorine analysis)
Nebulizer	MicroMist™ nebulizer 400 µL·min^{-1}		
Peristaltic pump tubing	PVC orange-green tubing, 0.38 mm i.d.		
Peristaltic pump speed	40 rpm		
Spray chamber	Quartz cyclonic, cooled at 2.7 °C		
Torch	Quartz torch		
Injector	2.5 mm i.d., Quartz		1.5 mm i.d., Quartz
Interface	Nickel sampler and skimmer cone with high sensitivity insert		
Plasma power	1,550 W		
Nebulizer gas	1.03 L·min^{-1}		0.72 L·min^{-1}
QCell setting	**He KED**	**TQ-O_2**	**TQ-O_2**
QCell gas flow	100% He 4.2 mL·min^{-1}	100% O_2 0.32 mL·min^{-1}	100% O_2 0.4 mL·min^{-1}
CR bias	-21 V	-6.3 V	-6.3 V
Q3 bias	-18 V	-12 V	-12 V
Scan setting	0.1 s dwell time, 5 sweeps, 3 main runs		2 s dwell time, 5 sweeps, 3 main runs
Analysis time per sample	Total 2 min 10 s: including uptake (40 s) and wash out (30 s)		1 min 40 s: including uptake (40 s) and wash out (30 s)

Sample preparation

Pre-cleaned polypropylene bottles were used for the preparation of all blanks, standards, and samples.

All blanks, calibration standards, spike recovery tests, and quality control (QC) solutions were prepared using a mixed solution with 1% v/v HNO_3 (Optima™ grade, Fisher Chemical™), 0.5% v/v HCl (Optima™ grade, Fisher Chemical™), and single-element stock standards (SPEX™ CertiPrep™, Metuchen, NJ, USA).

Table 2. Summary of the concentration details of the standard calibration, CCV (continuing calibration verification), and matrix (1,000 µg·L^{-1} phosphorus, yttrium, zirconium, palladium, and platinum solution) spike recovery test. All numbers are shown in µg·L^{-1}.

Element	Concentration range	QC CCV (n=3)	Spike value (n=3)
S, P, Li, Be, Fe, Ni, Cu	1–100	2.5	2.5
F	150–1,000	250	250
Others	0.01–100	0.025	0.025

Results and discussion

Sensitivity and linearity

Table 3 summarizes the Background Equivalent Concentration (BEC), instrument detection limit (IDL), and correlation coefficient (R^2) obtained for each of the 52 elements analyzed in this study. The IDLs were calculated as three times the standard deviation of ten replicate measurements of the calibration blank. This table also includes QC results (CCV, spike recovery) for all the target analytes. All numbers are shown in µg·L^{-1}. The analysis of phosphorous and sulfur in particular are significantly improved using the TQ-O_2 mode as it eliminates the commonly observed abundant polyatomic interferences and, in the case of sulfur, allows the most abundant isotope, ^{32}S (with a natural abundance of 95%), to be used for the measurement (via $^{32}S.^{16}O^+$). The QC CCV and spike recovery results both demonstrated excellent recovery of 89% to 107% for all the elements analyzed.

Comparing the analysis results of the He KED and TQ-O_2 modes for P and S shows that TQ-O_2 mode achieved superior calibration linearity with substantially improved detection limits. While He KED mode provided excellent performance in the mid and high mass range, it was not effective for phosphorous and was not able to provide a linear response in the selected calibration range for sulfur. As mentioned before, bias on the results for sulfur could be induced by the presence of higher levels of phosphorous due to the formation of $^{31}P^1H^+$ as an additional contribution on $^{32}S^+$. However, as demonstrated by the spike recovery results, the TQ-O_2 mode fully eliminated the $^{31}P^1H^+$ polyatomic interference even in the presence of up to 1,000 µg·L^{-1} of phosphorus.

In addition, typical catalyst materials used in fuel cells include elements such as yttrium, zirconium, and palladium alloyed with platinum, which again can lead to a series of both polyatomic as well as isobaric (isotopes of different elements with the same mass) overlaps for other critical analytes. In this case as well, TQ-O_2 mode eliminated these polyatomic interferences and enabled determination of the analysis results in an interference free region (Figure 2). Further to reducing polyatomic interferences, both first (Q1) and third quadrupoles (Q3) were set to high resolution by virtue of user definable resolution settings provided by the Qtegra ISDS Software, removing any potential peak tailing interference from neighboring high intensity signals.

Table 3. Summary of analysis mode, calibration results, BEC, IDL, R^2, CCV, and spike recovery for all analytes. Spike recoveries of the elements P, Y, Zr, Pd, and Pt were not evaluated as these were present at high concentrations (1,000 µg·L^{-1}) in the spike matrix test solution.

						CCV (n=3)		Spike recovery test (n=3)	
Analyte	Analysis mode	Q3 analyte	BEC (µg·L^{-1})	IDL (µg·L^{-1})	R^2	Recovery (%)	RSD (%)	Recovery (%)	RSD (%)
^{7}Li	TQ-O_2	^{7}Li	0.001	0.012	0.9999	93.8	0.8	98.5	2.8
^{9}Be	TQ-O_2	^{9}Be	<0.001	<0.001	0.9999	105.3	1.4	107.1	2.2
^{11}B	TQ-O_2	^{11}B	0.049	0.039	>0.9999	102.3	2.1	93.5	1.8
^{27}Al	TQ-O_2	^{27}Al	0.087	0.043	>0.9999	98.7	2.4	101.8	0.2
^{31}P	**He KED**	**-**	**2.411**	**1.898**	**0.9988**	**98.3**	**5.9**	-	-
^{31}P	TQ-O_2	^{31}P.^{16}O	0.064	0.017	0.9998	100	2.7	-	-
^{32}S	TQ-O_2	^{32}S.^{16}O	0.819	0.032	0.9996	99.6	2.5	103.2	2.3
^{34}S	**He KED**	**-**	**151.59**	**31.582**	-	**335**	**13.2**	1481	2.5
^{48}Ti	TQ-O_2	^{48}Ti.^{16}O	0.004	0.004	>0.9999	100.2	2.5	89.9	0.9
^{51}V	TQ-O_2	^{51}V.^{16}O	<0.001	0.001	>0.9999	98.2	2.4	92.1	1.1
^{52}Cr	TQ-O_2	^{52}Cr.^{16}O	0.039	0.018	>0.9999	98.7	2.4	105.4	1.6
^{55}Mn	He KED	-	0.001	0.002	>0.9999	105	2.5	93.4	1
^{56}Fe	He KED	-	0.184	0.046	0.9998	101.4	2.5	95.1	1
^{59}Co	TQ-O_2	^{59}Co	<0.001	0.001	>0.9999	99.7	2.2	91.8	1.3
^{60}Ni	He KED	-	0.014	0.009	>0.9999	106.1	2.5	93.4	0.9
^{63}Cu	He KED	-	0.006	0.003	>0.9999	105.7	2.6	93.6	1.3
^{66}Zn	He KED	-	0.027	0.012	0.9996	104.1	1.7	106.7	0.5
^{71}Ga	He KED	-	<0.001	0.001	>0.9999	105.9	2.1	93.2	1
^{72}Ge	He KED	-	<0.001	0.001	>0.9999	103	2.5	96.1	1.8
^{75}As	TQ-O_2	^{75}As.^{16}O	0.001	0.001	0.9999	104.6	1.9	101	1
^{80}Se	TQ-O_2	^{80}Se.^{16}O	0.001	0.004	0.9998	107.2	1.8	106.4	0.8
^{85}Rb	He KED	-	<0.001	0.001	>0.9999	105.6	1.4	94.1	2
^{88}Sr	TQ-O_2	^{88}Sr.^{16}O	0.001	0.002	>0.9999	98.7	0.5	91.2	1.4
^{89}Y	TQ-O_2	^{89}Y.^{16}O	<0.001	<0.001	>0.9999	99.7	1.1	-	-
^{90}Zr	TQ-O_2	^{90}Zr.^{16}O	0.003	0.003	>0.9999	97.7	4.5	-	-
^{98}Mo	TQ-O_2	^{98}Mo.^{16}O	0.001	0.002	>0.9999	100.1	1.4	95.7	0.7
^{101}Ru	He KED	-	<0.001	<0.001	>0.9999	104.5	0.9	93.4	1.1
^{103}Rh	He KED	-	<0.001	<0.001	>0.9999	105.6	1.3	95	0.4
^{107}Ag	TQ-O_2	^{107}Ag	0.001	<0.001	>0.9999	105.2	2.9	104.6	0.6
^{108}Pd	TQ-O_2	^{108}Pd	0.001	0.001	>0.9999	101	1.1	-	-
^{111}Cd	TQ-O_2	^{111}Cd	<0.001	<0.001	>0.9999	103.3	2.1	97.6	1.5
^{115}In	He KED	-	<0.001	<0.001	>0.9999	105.7	0.8	95.4	1.4
^{118}Sn	He KED	-	0.002	0.002	>0.9999	106.4	2.8	96	1.1
^{121}Sb	TQ-O_2	^{121}Sb	0.001	0.001	>0.9999	104.9	3	97.5	1.1
^{139}La	He KED	-	<0.001	<0.001	>0.9999	104.5	0.7	96.1	0.8
^{140}Ce	TQ-O_2	^{140}Ce.^{16}O	<0.001	<0.001	>0.9999	99.6	0.4	91.2	0.8
^{144}Nd	TQ-O_2	^{144}Nd.^{16}O	<0.001	<0.001	>0.9999	100	0.8	90.4	0
^{149}Sm	TQ-O_2	^{149}Sm.^{16}O	<0.001	<0.001	>0.9999	99.2	1.3	91.3	0.3
^{153}Eu	He KED	-	<0.001	<0.001	>0.9999	104.7	1.6	95.9	2.2
^{159}Tb	TQ-O_2	^{159}Tb.^{16}O	<0.001	<0.001	>0.9999	99.9	0.4	91.6	0.6
^{172}Yb	He KED	-	<0.001	<0.001	>0.9999	104.2	0.8	95.8	0.6
^{175}Lu	TQ-O_2	^{175}Lu.^{16}O	<0.001	<0.001	>0.9999	99	0.5	91.9	0.6
^{178}Hf	TQ-O_2	^{178}Hf.^{16}O	<0.001	<0.001	>0.9999	101	2.3	95.4	0.1

Continued on next page

Table 3 (continued from previous page). Summary of analysis mode, calibration results, BEC, IDL, R^2, CCV, and spike recovery for all analytes. Spike recoveries of the elements P, Y, Zr, Pd, and Pt were not evaluated as these were present at high concentrations (1,000 µg·L^{-1}) in the spike matrix test solution.

						CCV (n=3)		Spike recovery test (n=3)	
Analyte	Analysis mode	Q3 analyte	BEC (µg·L^{-1})	IDL (µg·L^{-1})	R^2	Recovery (%)	RSD (%)	Recovery (%)	RSD (%)
^{181}Ta	TQ-O_2	^{181}Ta.^{16}O	<0.001	0.001	>0.9999	97.4	3.5	95.7	1
^{182}W	He KED	-	<0.001	<0.001	>0.9999	109.3	22	99.1	1
^{185}Re	He KED	-	<0.001	<0.001	>0.9999	105	0.8	96.6	0.9
^{193}Ir	He KED	-	<0.001	<0.001	>0.9999	106.4	0.5	98.4	1.1
^{194}Pt	He KED	-	0.007	0.002	>0.9999	107.1	2.6	-	-
^{197}Au	TQ-O_2	^{197}Au	0.005	0.002	>0.9999	105.4	4.2	102.1	1.1
^{205}Tl	He KED	-	<0.001	<0.001	>0.9999	105.4	3.3	98.1	0.4
^{208}Pb	He KED	-	<0.001	<0.001	>0.9999	105.1	6.5	97.9	1.2
^{209}Bi	He KED	-	0.001	<0.001	>0.9999	108.2	1.7	98.8	0.6
^{232}Th	He KED	-	<0.001	<0.001	>0.9999	101.9	1.7	94.1	0.8
^{238}U	He KED	-	<0.001	<0.001	>0.9999	104	1.3	96.3	0.8

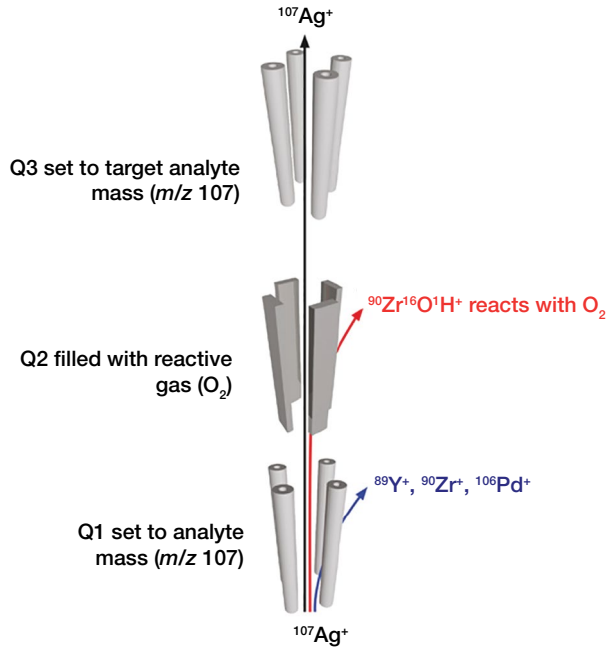

Figure 2. Schematic showing the use of TQ-O_2 mode and a mass shift reaction for interference free detection of silver (Ag)

To evaluate the application of high resolution on Q1 and Q3, a 1,000 µg·L^{-1} solution of the matrix analytes P, Y, Zr, Pd, and Pt, plus 1,000 µg·L^{-1} S was used for monitoring potential interferences, either caused by peak tailing from the abundant signals of adjacent isotopes or polyatomic interferences.

Table 4 shows the comparison of the results obtained for the analysis of solutions containing 1,000 µg·L^{-1} sulfur, yttrium, zirconium, palladium, and platinum, respectively, between the He KED and TQ-O_2 modes. TQ-O_2 mode fully removed the polyatomic interferences and provided significantly lower blank equivalent concentrations. It is noteworthy that the platinum standard solution used for this test contained a small amount of gold as an impurity, and the measured BEC is in line with the expected concentration. Also, increased backgrounds due to peak tailing from adjacent Pt isotope signals were not observed, even though the signal measured at *m/z* 196 exceed the signal at *m/z* 197 by several orders of magnitude. This demonstrates the superior abundance sensitivity of the system.

Table 4. Blank equivalent concentrations for sulfur, silver, cadmium, and gold in presence of key interferents (all data are in µg·L^{-1})

	Interference	He KED	TQ-O_2
Sulfur	i.e., $^{16}O^{16}O$	38 at ^{34}S	0.062 at ^{32}S
^{107}Ag	i.e., $^{91}Zr^{16}O^+$	0.160	0.003
^{111}Cd	i.e., $^{94}Zr^{16}O^1H^+$ or $^{110}Pd^1H^+$	0.065	0.003
^{197}Au	$^{196}Pt^1H$	0.015	0.013

Analysis of fluorine

The analysis of fluorine is important for evaluating the degradation of the polymeric membrane used in a hydrogen fuel cell; however, it is very challenging to determine this element using ICP-MS. In this study, an alternative approach, previously described by Jamari et al.[1], for the analysis of fluorine was applied. In short, 30 mg·L^{-1} of barium (Ba) is spiked into the fluorine analysis solutions before entering the plasma. Subsequently, BaF is formed and measured at *m/z* 157. This approach helps to mitigate the challenge of poor ionization. However, quantitative formation of BaF^+ while simultaneously preventing it from decomposing is critical and challenging. In addition, *m/z* 157 also suffers significantly due to barium-based polyatomic interferences, including $^{138}Ba^{16}O^3H$, as well as other Ba, O, and H combinations. Therefore, analysis of fluorine using this approach is only feasible when using triple quadrupole ICP-MS.

To tackle this challenge and perform interference-free analysis of F as BaF^+, the iCAP TQe ICP-MS was operated using TQ-O_2 mode with mass measurement of BaF at *m/z* 157. Figure 3 shows the settings applied for Q1 and Q3 together with the relevant ions and reactions.

To verify the performance of the system, a spike recovery test was performed at a concentration of approximately 10 times the instrumental detection limit. The results are summarized in Table 5. As can be seen, the detection of fluorine is in principle feasible, and a detection limit of approximately 30 µg·L^{-1} could be achieved. The measurements were proven reproducible by means of a continuing calibration verification test, performed at a concentration level of 250 µg·L^{-1}.

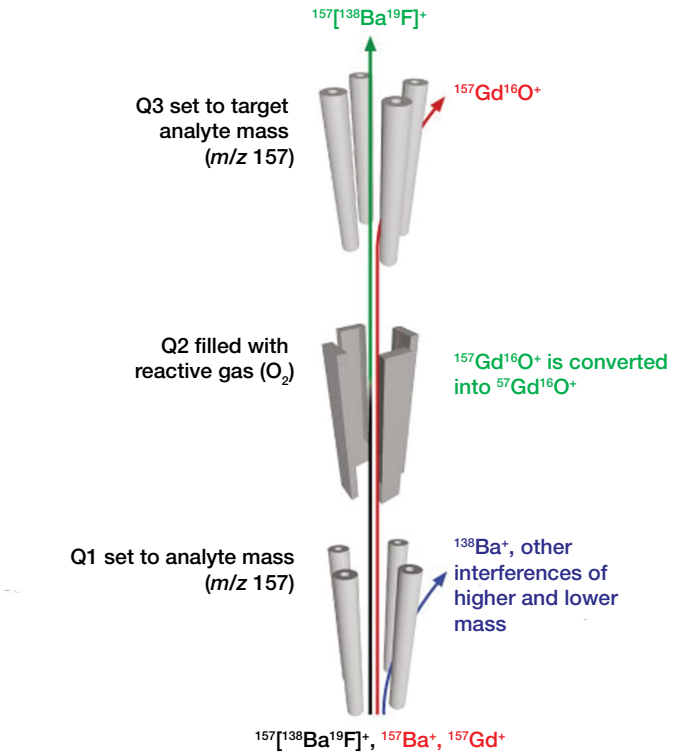

Figure 3. Schematic showing the use of TQ-O_2 mode and a mass shift reaction for interference free detection of fluorine after reaction with barium

Table 5. Analytical figures of merit for the analysis of fluorine after formation of BaF

Analyte	Analysis mode	Q3 analyte	LOD (µg·L^{-1})	Correlation coefficient	CCV (n=3)
^{19}F	TQ-O_2	$^{138}Ba^{19}F$	30	0.9995	107 ± 2.0

Conclusions

The iCAP TQe ICP-MS was employed to analyze 53 elements including fluorine in process water derived from hydrogen fuel cells. Among the analytes, several critical interferences can cause unexpected bias, and these were investigated closely for effective and complete removal by means of selective collision / reaction cell reactions with oxygen. This study also included the development of a method for the analysis of fluorine, generally only possible in an indirect measurement. This analytical method was rigorously tested, and the results obtained clearly demonstrate the fowling analytical advantages:

- The iCAP TQe ICP-MS operated in TQ-O_2 and He KED modes allowed the analysis of 53 elements in relevant sample matrices over a wide concentration range. For minor elements, the method was tested over 4 orders of magnitude (from 0.01 to 100 µg·L^{-1}), whereas major elements were tested between 1 to 100 µg·L^{-1}.
- Using a high throughput analysis approach, with a new autosampler equipped with a Step Ahead feature for minimizing total analysis time, all elements relevant for the development of hydrogen fuel cell technology could be measured accurately with low detection limits.
- The use of TQ-O_2 mode provided advanced performance for eliminating the polyatomic interferences of phosphorus, sulfur, silver, and cadmium in the simulated hydrogen fuel cell process water. This covered both polyatomic interferences as well as overlaps created by intense signals from isotopes of elements present in high concentrations.
- The iCAP TQe ICP-MS offers the flexibility to choose high resolution for the Q1 and Q3 quadrupoles, enabling complete elimination of polyatomic interference and isobaric interferences.
- The feasibility of fluorine analysis was demonstrated using an indirect method after complexation with barium. The iCAP TQe ICP-MS showed accurate and precise determination of fluorine as proven by the spike recovery tests performed.
- Excellent stability performance was obtained with the iCAP TQe ICP-MS together with excellent CCV and spike recovery results over a 3-hour run without internal standard correction. This provides the advantage of avoiding potential contamination from addition of the internal standard solution.

Reference

1. N. Laili, N.; Jamari. A.; et al. Novel non-target analysis of fluorine compounds using ICPMS/MS and HPLC-ICPMS/MS. *Journal of Analytical Atomic Spectrometry,* **2017,** *32,* 42–950.

Learn more at **thermofisher.com/icp-ms**